1-1-1990

Multiconfiguration Hartree-Fock Calculation Of The Photoionization Of The Cs 7D Excited-State

H. P. Saha

University of Central Florida

Recommended Citation

Saha, H. P., "Multiconfiguration Hartree-Fock Calculation Of The Photoionization Of The Cs 7D Excited-State" (1990). *Faculty Bibliography 1990s*. 138.
https://stars.library.ucf.edu/facultybib1990/138

PHYSICAL REVIEW A VOLUME 41, NUMBER 1 1 JANUARY 1990

Multiconfiguration Hartree-Fock calculation of the photoionization of the Cs 7*d* excited state

H. P. Saha
Department of Physics, University of Central Florida, Orlando, Florida 32816-0993

(Received 21 August 1989)

The numerical multiconfiguration Hartree-Fock method is used to calculate the photoionization cross section for the Cs 7*d* excited state. The electron correlation and the dynamical core-polarization effects, which are very important for photonioization-cross-section calculations of the cesium atom, have been taken into account in an *ab initio* manner through the configuration-interaction procedure. A minimum has been found in the total photoionization cross section. The calculation of the photoionization angular-distribution asymmetry parameter is proved to be an excellent test to determine the existence and location of the minimum in the cross section. The length and velocity forms of the cross section and the asymmetry parameter are found to be in excellent agreement over the entire incident photon energy range considered, suggesting that converged results may be obtained in this interval with the present approach. The results obtained are compared with the recent experimental measurements of the absolute photoionization cross section and are found to be in good agreement.

I. INTRODUCTION

The alkali-metal atoms are currently receiving considerable attention,[1] especially those processes involving promotion of one electron outside the closed core. With respect to many processes, these electrons can be assumed to act independently of the core, and they are notorious for being strongly correlated.[2] Photoionization cross sections of alkali-metal atoms in the excited state have long provided a computational challenge to the theorist. The polarization of the core by the valence electron generally requires studies beyond the Hartree-Fock approximation. Moreover, the final-state continuum functions are also affected by the polarizability of the remaining ionic core. In recent years various calculations have predicted the existence of minima in the photoionization cross section of the excited states of atoms.[3-6] These minima arise when matrix elements as a function of the ejected electron energy change their sign in the $l \rightarrow l+1$ or $l \rightarrow l-1$ channels. These minima are very sensitive to the details of the initial- and the final-state wave functions and as such provide an excellent test of the approximation methods when compared with experiment.

Cesium is the most interesting of the alkali metals because electron-election correlation and core-polarization effects are largest for this atom. Recent experiments[7,8] have been performed on the photoionization of the excited states of cesium atom. Gerwert and Kollath[7] measured relative photoionization cross section for the $7\,^2P_{3/2}$ and $6\,^2D_{3/2}$ excited states of cesium in the visible spectral range of the ionizing photon. The measurement was performed using two pulsed dye lasers, pumped by the same excimer laser, for population of the excited states and for their photoionization. Very recently Bonin *et al.*[8] measured absolute photoionization cross sections from the excited $7\,^2D_{3/2}$ state of cesium. Their technique involves utilization of a simple measurement of the reduction in the excited-atom fluorescence due to photoionization. This method is different from the other experiments on the excited-state cross section in that past experiments generally relied on measurements of the total number of ions or photoelectrons produced by photoionization. Various theoretical calculations have been reported on photoionization from the excited states of cesium atom. Lahiri and Manson[9] performed calculation on the photoionization cross section from the Cs 6*d* excited state. They used Hartree-Slater central-field approximation and obtained a minimum in the total cross section near the threshold. Later Msezane and Manson[10] applied the Hartree-Fock method to obtain the photoionization cross section from the excited state of cesium. They again found a minimum in the cross section but at a higher energy. These results agree very well with the relative cross section measured by experiment.[7] Avdonina and Amusia calculated photoionization cross sections from the *nd* ^2D states of cesium. They used random phase approximation with exchange to obtain photoionization cross section. They compared these results with that obtained with other approximations and found that results are sensitive to the choice of used approximations.

Recently Saha *et al.*[11] applied the multiconfiguration Hartree-Fock (MCHF) method[12] to the calculation of the partial photoionization cross section from the excited 4*d* subshell of sodium in the energy region from 0.0 to 13.6 eV, employing procedures that allow optimization at each kinetic energy of the important core-polarization effects on the continuum function as well as for the incorporation of target and the ionic core configuration mixing effects. In this paper we report a calculation on the photoionization cross section from the excited $7\,^2D$ state of cesium. The method we used is the multiconfiguration

Hartree-Fock method applied earlier to the calculation of photoionization cross section from the excited 4*d* state of sodium. The calculations have been performed using both the Hartree-Fock (HF) and the more sophisticated MCHF method to calculate wave functions for the initial excited discrete state and the final continuum state. The main emphasis in this investigation is to take into account the electron correlation and the dynamical core-polarization effects *ab initio* in order to obtain an accurate photoionization cross section and compare them with the recent experimental measurement.[8]

II. THEORY

A. Photoionization cross sections

In the dipole approximation the photoionization cross section for a transition from an initial state i to a final state f is given by

$$\sigma(\omega)=4\pi^2\alpha a_0^2\omega\sum_{f,m}|\langle\psi_f|T|\psi_i\rangle|^2 .$$

The operator T is the dipole transition operator given by

$$T=T_L=\sum_{j=1}^{n}Z_j$$

in the length form and

$$T=T_V=\sum_{j=1}^{n}\frac{\nabla_j^z}{i\omega}$$

in the velocity form. The matrix elements

$$M=\langle\psi_f|T|\psi_i\rangle$$

are evaluated in atomic units. α is the fine-structure constant and a_0 is the Bohr radius of the hydrogen atom. ω is the energy of the incident photon in a.u. ψ_i and ψ_f are, respectively, the initial- and the final-state wave functions and the sums run over the configurations f and all magnetic quantum numbers m. When ψ_i and ψ_f are exact solutions of the same Hamiltonian equations, the length and the velocity forms of the cross section will be identical.

B. Asymmetry parameters $\beta_{nl}(\omega)$

The angular distribution of photoelectrons ionized from a particular excited subshell nl by light polarized in the $\hat{\mathbf{e}}$ direction is related to the differential cross section for photoionization at energy ω by the relation[13]

$$\frac{d\sigma_{nl}(\omega)}{d\Omega}=\frac{\sigma_{nl}(\omega)}{4\pi}[1+\beta_{nl}(\omega)P_2(\hat{\mathbf{e}}\cdot\hat{\mathbf{k}})] ,$$

where $\sigma_{nl}(\omega)$ is the total photoionization cross section at energy ω corresponding to the electron ionized from the excited subshell nl. P_2 is the second-order Legendre polynominal, whose argument is the cosine of the angle between the polarization vector $\hat{\mathbf{e}}$ of the incident radiation and the direction $\hat{\mathbf{k}}$ of the photoelectron momentum, and $d\Omega$ is the solid angle into which the photoelectron is scattered. The asymmetry parameter is a function of ω, arising because of interference between various final states of the ion plus photoelectron. The parameter $\beta_{nl}(\omega)$ is more sensitive to the behavior of the photoionization amplitude and the phase shifts than the total or even the partial cross section.

In the Cooper-Zare model, the asymmetry parameter $\beta_{nl}(\omega)$ is given by[14]

$$\beta_{nl}(\omega)=\frac{l(l-1)T_{l-1}^2(\omega)+(l+1)(l+2)T_{l+1}^2(\omega)-6l(l+1)T_{l-1}(\omega)T_{l+1}(\omega)\cos(\xi_{l+1}-\xi_{l-1})}{(2l+1)[lT_{l-1}^2(\omega)+(l+1)T_{l+1}^2(\omega)]} ,$$

where $T_{l-1}(\omega)$ and $T_{l+1}(\omega)$ are the radial parts of the dipole matrix element corresponding to the $l-1$ and $l+1$ channels, respectively, and $\xi_l(\omega)$ is the total phase shift of the lth channel.

C. MCHF wave function for a continuum state

The MCHF wave function for a continuum state may be expressed in terms of a single continuum orbital coupled to a wave function for an N-electron core and the other bound $(N+1)$-electron configuration state.

Let

$$\psi(\gamma_c L_c S_c;N)=\sum_{j}^{m_c}a_j\Phi(\gamma_j L_c S_c;N)$$

be a wave function describing an N-electron core that is an eigenstate of L_c and S_c, in terms of N-electron bound configuration states $\Phi(\gamma_j L_c S_c;N)$ with configuration γ_j and term L_cS_c, mixing coefficients a_j, and the total energy E_c. Let ϕ_{kl} be a one-electron, continuum orbital with orbital angular momentum l. Then a MCHF wave function for a continuum state with label γ, energy E, and term LS may be expressed in a series of the form

$$\Psi(\gamma LS;N+1)=\sum_{j=1}^{m_c}a_j\Phi(\gamma_j L_c S_c;N)\phi_{kl}+\sum_{i=1}^{m}C_i\Phi(\gamma_i LS;N+1) ,$$

where $\Phi(\gamma_j L_c S_c;N)\phi_{kl}$ represents the coupling of the N-electron configuration with a single electron to yield an antisymmetric configuration state for the $(N+1)$-electron system with the designated final term value and configuration $\gamma_j kl$. The second term is the sum of $(N+1)$-electron bound-state configurations which are eigenstates with the same L and S and which are included to allow for electron correlation and the core polarization.

The MCHF method for continuum states assumes all the radial functions describing the core are fixed, along with the mixing coefficients a_j. Other bound-state radial functions may be determined variationally along with the radial function for the continuum electron. A set of radial function $P_i(r)$, $i=1,\ldots,m$, which defines the above MCHF wave function, is a solution of the coupled integro-differential equation of the form

$$\left[\frac{d^2}{dr^2}+\frac{2Z}{r}-\frac{l(l+1)}{r^2}\right]P_i(r) = \frac{2}{r}[Y_i(r)P_i(r)+X_i(r)+I_i(r)]+\sum_{i'}\varepsilon_{ii'}P_{i'}(r)\ .$$

The off-diagonal energy parameters $\varepsilon_{ii'}$ are related to Lagrange multipliers to ensure orthogonality assumptions. In the equation $(2/r)Y_i(r)$ is the screening potential, $(2/r)X_i(r)$ is the exchange function, and $(2/r)I_i(r)$ represents terms arising from interactions between configuration states.

Bound radial function satisfy the boundary conditions,

$$P_i(r)\xrightarrow[r\to 0]{} r^{l+1} \text{ and } P_i(r)\xrightarrow[r\to\infty]{} 0\ .$$

In this case the diagonal energy parameter ε_{ii} is an eigenvalue of the integro-differential equation and hence needs to be determined. The radial functions for the continuum orbital satisfy the conditions

$$P_i(r)\xrightarrow[r\to 0]{} r^{l+1}\ ,$$

$$P_i(r)\xrightarrow[r\to\infty]{}\left[\frac{2}{\pi k}\right]^{1/2}\sin\left[kr-\frac{l\pi}{2}+\frac{q}{k}\ln(2kr)+\sigma_l+\delta_l\right]\ ,$$

where $\sigma_l=\arg[(l+1-iq/k)]$ is the Coulomb phase shift, δ_l is the residual phase shift, $q=Z-N$ is the net charge of the ion, and $\varepsilon_{ii}=-k^2$, k^2 being the kinetic energy of the continuum electron.

The coupled integro-differential equations are solved numerically by the iterative method. The multiconfiguration (MC) self-consistent-field (SCF) procedure is applied to compute both the bound and the continuum wave functions. The same numerical procedures are used for both the bound and the continuum wave functions. The bound radial functions are essentially bound in nature and vary smoothly as $r\to\infty$. The continuum radial function is obtained by outward integration only, there being no exponentially decaying "tail" region. The continuum radial function was normalized by fitting the computed values at two adjacent points to the regular and irregular Coulomb functions as soon as the Coulomb region is reached. The coefficients C_i are solutions of the system of equations

$$\sum_{i'=1}^{m}\langle\Phi_i|H-E|\Phi_{i'}\rangle C_{i'}+\sum_{j=1}^{m_c}\langle\Phi_i|H-E|\Phi_j\rangle a_j=0\ ,$$
$$i=1,\ldots,m$$

where

$$\Phi_j=\Phi(\gamma_j L_c S_c;N)\phi_{kl}\ ,\quad j=1,\ldots,m_c$$

and

$$\Phi_i=\Phi(\gamma_i LS;N+1),\quad i=1,\ldots,m\ .$$

H is the Hamiltonian for the $(N+1)$-electron system and $E=E_c+k^2/2$ (in a.u.).

III. COMPUTATIONAL PROCEDURE

In our calculation we consider the process

$$\hbar\omega+\mathrm{Cs}(5s^25p^67d\ ^2D)\rightarrow\mathrm{Cs}^+(5s^25p^6\ ^1S)+e^-(kp)\ ^2P^\circ$$
$$\rightarrow\mathrm{Cs}^+(5s^25p^6\ ^1S)+e^-(kf)\ ^2F^\circ\ .$$

The accuracy of the photoionization cross section depends on two factors: (1) accurate calculation of threshold energy and (2) accurate calculation of the dipole matrix element whose accuracy again depends on the wave function of the initial and final states. As stated earlier, the electron-electron correlation and the dynamical core-polarization effects are very important for the photoionization cross section of the Cs $7d$ excited state. Two sets of calculations are performed in order to study the effect of core polarization and the electron correlation by the valence electron in the initial state and by the continuum electron in the final state. In the HF calculation, which neglects the electron correlation and the polarization effects, both the initial and the final states are represented by the single configuration. In the MCHF calculation, which considers the electron correlation and polarization effects very accurately, all the configurations contributing to these effects are included. To simplify the evaluation of the electric dipole transition-matrix elements, the $1s$, $2s$, $2p$, $3s$, $3p$, $3d$, $4s$, $4p$, $4d$, $5s$, and $5p$ radial functions for both the states are obtained from the HF calculation of the core $5s^25p^6\ ^1S$ state.

A. Initial-state wave function $5s^25p^67d\ ^2D$

The initial bound-state wave function is calculated by the multiconfiguration Hartree-Fock method.[15] The MCHF wave-function expansion was over the set of 23 configuration states coupled to form a ^2D term:

$$\{5s^25p^67d,5s^25p^55d6p,5s^25p^56s6p,5s^25p^56p6d\ ,$$
$$5s5p^65d6s,5s5p^66s6d,5s5p^65d^2,5s5p^65d6d\ ,$$
$$5s5p^66p^2,5s5p^66d^2\}^2D\ .$$

The above expansion represents the set of configurations whose contribution towards the dipole matrix element is appreciable. The initial-state wave function is obtained by MCHF calculation varying five orbitals simultaneously.

B. Final-state wave function

1. $5s^25p^6kp\ ^2P^\circ$

The final MCHF wave-function expansion was over the set of 36 configurations coupled to form a $^2P^\circ$ term:

$$\{5s^2 5p^4 6P_2^3, 5s^2 5p^4 5d^2 6p_2, 5s^2 5p^4 6s^2 6p_2\ , 5s^2 5p^6 kp_1\}^2P^\circ\ .$$

The radial functions $5d$, $6s$, $6p_2$, and kp_1 are varied simultaneously at each kinetic energy of the photoelectron.

2. $5s^2 5p^6 kf\ ^2F^\circ$

For the final continuum state $5s^2 5p^6 kf\ ^2F^\circ$, the MCHF expansion was over the set of 41 configuration states:

$$\{5s 5p^6 5d 6p_2, 5s 5p^5 5d 6p_2^2, 5s 5p^5 6s 6p_2^2, 5s^2 5p^5 5d 6s\ ,$$
$$5p^6 5d^2 6p_2, 5s^2 5p^4 5d 6s 6p_2, 5s^2 5p^4 5d^2 6p_2\ ,$$
$$5s^2 5p^4 6s^2 6p_2, 5s^2 5p^4 6p_2^3, 5s^2 5p^6 kf_1\}^2F^\circ\ .$$

In this expansion three bound radial functions $5d, 6s, 6p_2$ and one continuum radial function kf_1 are varied simultaneously at each kinetic energy of the photoelectron. In all cases $1s$, $2s$, $2p$, $3s$, $3p$, $3d$, $4s$, $4p$, $4d$, $5s$, and $5p$ wave functions are kept fixed at the HF $5s^2 5p^6\ ^1S$ value.

IV. RESULTS

The calculated photoionization HF threshold energy is 0.6338 eV and the MCHF threshold energy is 0.6489 eV. The MCHF threshold energy compares very well with the experimental[16] value 0.6625 eV. In all the cross-section calculations we used the experimental threshold energy.

A. Photoionization cross section

In the HF approximation, the partial photoionization cross section for the $7d \rightarrow kf$ transition is calculated in both the length and velocity forms for photoelectron energies from threshold to 2.5 Ry. At threshold this cross section is large and decreases rapidly near the threshold and then slowly as the energy increases. This cross section approaches zero at about 0.99 Ry (length) and 0.96 Ry (velocity), after which the cross section increases again and goes to a maximum at about 1.50 Ry (length) and 1.45 Ry (velocity). With the further increase of energy, the cross section decreases slowly. There is a considerable difference in the length and velocity cross sections, particularly near the threshold and around the region where the cross section goes to zero.

The partial photoionization cross section for the $7d \rightarrow kp$ transition is calculated in the HF approximation in both the length and the velocity forms for the same energy range. In this transition, the cross section decreases from the threshold and goes to zero at about 0.30 Ry (length) and 0.60 Ry (velocity), after which it increases again and goes to a maximum at about 0.97 Ry (length) and 1.65 Ry (velocity). The cross section decreases with the further increase of energy. There is a considerable difference between the HF length and HF velocity cross sections in this transition; the difference increases with the increase of energy.

The partial photoionization cross section for the $7d \rightarrow kf$ transition is calculated in the MCHF approximation in both the length and velocity forms for the same range of energy. This cross section has the similar qualitative structure as the corresponding quantities in the HF approximation. In this case the cross section decreases and goes to a zero at about 0.98 Ry (length) and 0.97 Ry (velocity), after which it increases to a maximum at about 1.50 Ry (length) and 1.49 Ry (velocity). The cross section decreases with the further increase of energy. The remarkable feature of the MCHF results is that the length and velocity cross sections are in excellent agreement throughout the range of energy considered, whereas in the HF approximation there is a considerable difference in the length and velocity results. The agreement between the length and velocity results in the MCHF approximation clearly supports the accuracy of the MCHF wave functions.

The partial photoionization cross sections for the $7d \rightarrow kp$ transition in the MCHF approximation show the same general qualitative behavior as that in the HF approximation. They are relatively large at threshold, decrease to a minimum, then increase and go to a maximum and decrease again. In this case the minimum occurs at 0.55 Ry (both length and velocity) and they go to a maximum at above 1.35 Ry (both length and velocity). The MCHF length and the velocity cross section in this transition also agree very well throughout the range of energy considered.

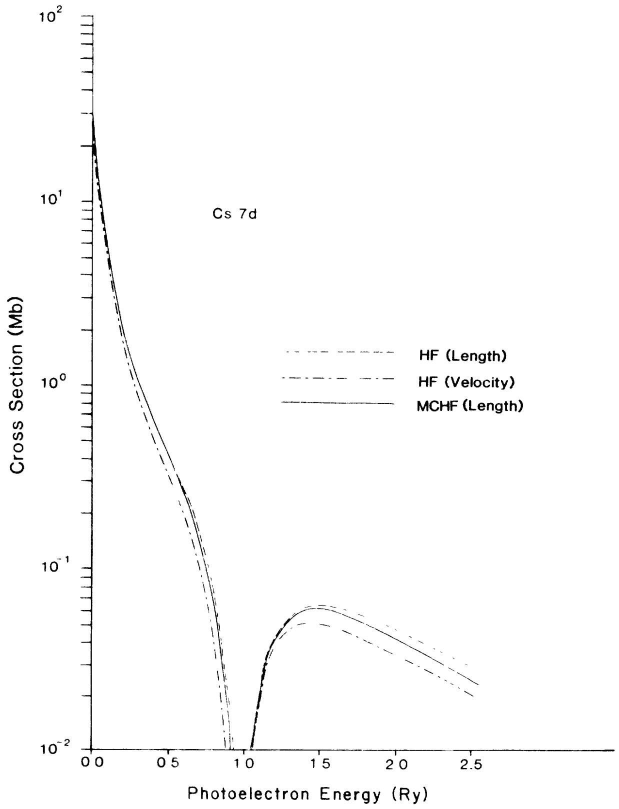

FIG. 1. Cs $7d$ photoionization cross sections as a function of photoelectron energy (Ry) using the Hartree-Fock (HF) and multiconfiguration Hartree-Fock (MCHF) wave functions.

Except for the narrow, near-threshold region, the $7d \rightarrow kp$ cross sections are very small compared to the $7d \rightarrow kf$ cross sections obtained in the HF and the MCHF approximation and do not contribute significantly to the total cross section.

The total cross section is obtained by summing up the two partial cross sections and is presented in Fig. 1 as a function of photoelectron energy. In the figure both HF length and velocity cross sections and the MCHF length cross sections are shown. As there is negligible difference between the MCHF length and the MCHF velocity cross sections, the MCHF velocity cross section is not shown in the figure. The HF length and velocity total cross sections go to a minimum at about 0.99 Ry (length) and 0.96 Ry (velocity) respectively, whereas the MCHF cross section goes to a minimum at about 0.98 Ry. The cross sections increase again and go to a maximum at about 1.50 Ry (HF length), 1.45 Ry (HF velocity), and 1.50 Ry (MCHF). With the further increase of energy, the cross sections decrease with the increase of energy. Comparing the MCHF total cross section with the HF total cross section, it is found that the MCHF cross sections do not differ significantly from the HF length cross section except near the threshold and around the cross-section minimum. The MCHF cross sections are lower than the HF cross section near the threshold and the minimum is shifted slightly towards the threshold.

In Fig. 2, the total cross sections obtained in the HF and MCHF approximations are shown as a function of photon energy along with the experimental points[8] in the energy region where the measurements have been made. As mentioned earlier, Bonin *et al.*[8] measured the absolute photoionization cross section using the techniques which utilize the simple measurement of the reduction in the excited-atom fluorescence due to photoionization. It is seen from the figure that there is a good agreement between the present results and the experiment over the small energy region where the absolute measurement have been made.

B. Asymmetry parameter $\beta_{nl}(\omega)$

The asymmetry parameter $\beta_{nl}(\omega)$ for the Cs $7d$ photoionization is shown in the Fig. 3, where the HF and the MCHF results are presented as a function of photoelectron energy. From the expression of the $\beta_{nl}(\omega)$, it is seen that at the point where the $7d \rightarrow kf$ cross section is zero, the photoelectron angular distribution asymmetry parameters $\beta_{nl}(\omega)$ must be equal to 0.2. The asymmetry parameter $\beta_{nl}(\omega)$ depends on the accuracy of the photoionization amplitude and the phase shifts. From the figure it is seen that the HF length and velocity reach $\beta=0.2$ at about 0.99 Ry (length) and 0.96 Ry (velocity), whereas the MCHF results show $\beta=0.2$ at about 0.98 Ry. On the

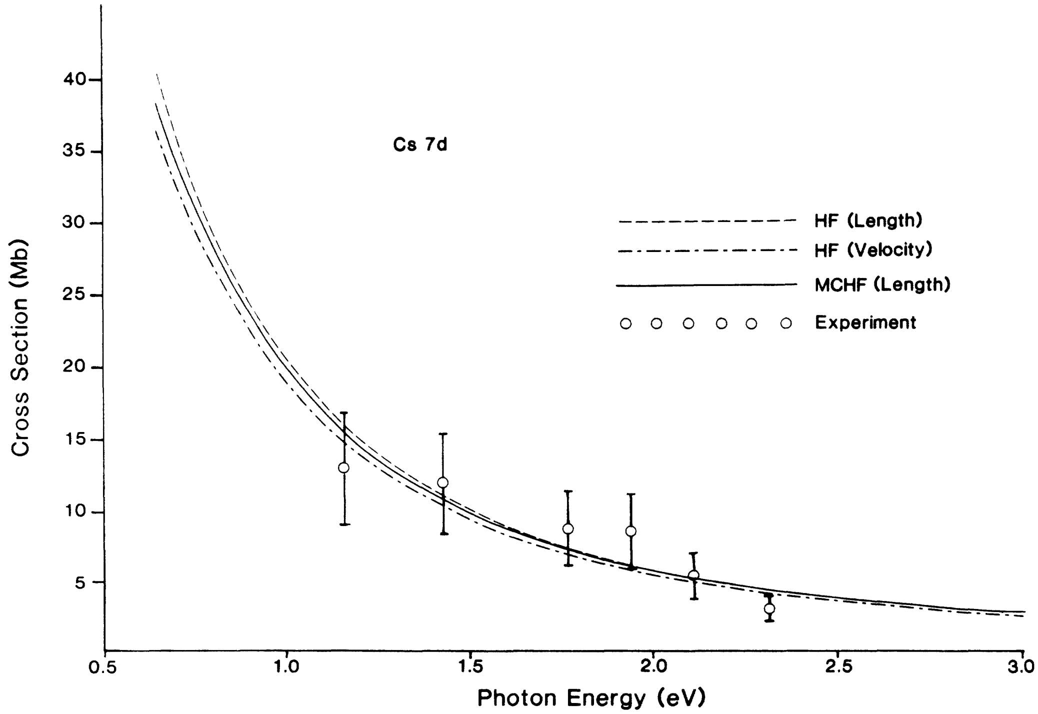

FIG. 2. Photoionization cross section for Cs $7d$ as a function of photon energy in the Hartree-Fock and the multiconfiguration Hartree-Fock approximation compared with experiment. The experimental results are from Ref. 8.

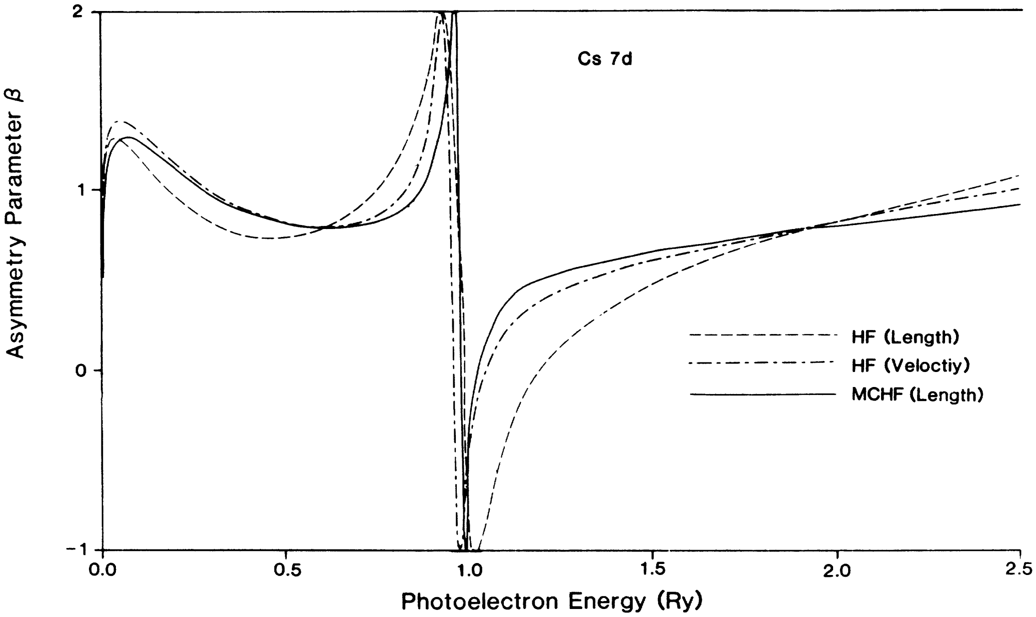

FIG. 3. Photoelectron angular distribution asymmetry parameter β for Cs $7d$ in both length and velocity formulations, using Hartree-Fock and multiconfiguration Hartree-Fock wave functions.

other hand, the value of $\beta_{nl}(\omega)$ will be equal to 0.8 where the cross section for the transition $7d \rightarrow kp$ goes to zero. It is seen from the figure that the HF length and velocity results reach $\beta=0.8$ at about 0.30 Ry (length) and 0.60 Ry (velocity) and the MCHF results show $\beta=0.8$ at about 0.55 Ry. The MCHF length and velocity results are nearly the same. As a result, in Fig. 3, we have shown only the MCHF length results. Although the partial photoionization cross sections for the $7d \rightarrow kp$ transition do not contribute significantly to the total cross sections, they are very important in the calculation of the photoelectron angular-distribution asymmetry parameter. The difference between the HF and MCHF results is due to the effect of core polarization and the electron correlation.

V. CONCLUSION

Extensive and careful studies of the photoionization cross section for the Cs $7d$ excited state have been performed using the multiconfiguration Hartree-Fock approximation. Short-range correlation and the long-range dynamical core-polarization effects which are very important for the photoionization cross section of the Cs atom have been taken into account adequately in an *ab initio* manner through the configuration-interaction procedures. The cross sections for the $7d \rightarrow kp$ transition are found to be very small compared to those for the $7d \rightarrow kf$ transition except the narrow near-threshold region. As a result the cross sections for the $7d \rightarrow kp$ transition do not contribute significantly to the total cross sections. Although the partial cross section for the $7d \rightarrow kf$ transition in the MCHF approximation does not change very much compared to that obtained in the HF approximation, the difference between the length and the velocity cross sections in the HF approximation is reduced almost completely in the MCHF approximation due to the inclusion of many configuration states which represent the electron correlation and the dynamical core polarization. The disagreement between the length and the velocity cross section for the $7d \rightarrow kp$ transition in the HF approximation also shows up in the photoelectron angular distribution asymmetry parameter. It is found that the present total cross sections agree well with the experimental results in the energy region where the measurements have been made. Excellent agreement between the MCHF length and velocity cross sections shows the accuracy of the initial- and the final-state wave functions. It should be mentioned that we do not consider the effects of spin-orbit interaction in the present calculation. We believe that spin-orbit interaction will not change the total photoionization cross-section results significantly except at the minimum. Finally, we conclude that the MCHF method which can take into account the correlation and the polarization effects very accurately and in an *ab initio* manner predicts reliable results.

ACKNOWLEDGMENTS

This research was supported by the National Science Foundation, under Grant No. PHY-8801881, and in part by a Cottrell Research Grant from the Research Corporation. Acknowledgment is also made to the donors of the Petroleum Research Fund, administered by the American Chemical Society, for partial support of this research. This research was also supported by the Florida State University Supercomputer Computations Research Institute, which is partially supported by the U.S. Department of Energy through Contract No. DE-FC05-85ER25000 and the Florida State University through time granted on its Cyber 205 Supercomputer.

[1] C. H. Greene and L. Kim, Phys. Rev. A **36**, 2706 (1987).

[2] H. N. Russell and F. A. Saunders, Phys. Rev. **61**, 38 (1925).

[3] A. Z. Msezane and S. T. Manson, Phys. Rev. Lett. **35**, 364 (1975).

[4] A. Z. Msezane and S. T. Manson, Phys. Rev. Lett. **48**, 473 (1982).

[5] J. Lahiri and S. T. Manson, Phys. Rev. Lett. **35**, 614 (1982).

[6] N. B. Avdonina and M. Ya. Amusia, J. Phys. B **16**, L543 (1983).

[7] K. Gerwert and K. J. Kollath, J. Phys. B **16**, L217 (1983).

[8] K. D. Bonin, M. Gatzke, C. L. Collins, and M. A. Kadar-Kallen, Phys. Rev. A **39**, 5624 (1989).

[9] J. Lahiri and S. T. Manson, in *Abstracts of Contributed Papers, Twelfth International Conference on the Physics of Electronic and Atomic Collisions, (Gatlinburg, Tennessee, 1981),* edited by S. Datz (North-Holland, Amsterdam, 1982), p. 89.

[10] A. Z. Msezane and S. T. Manson, Phys. Rev. A **29**, 1594 (1984).

[11] H. P. Saha, M. S. Pindzola, and R. N. Compton, Phys. Rev. A **38**, 128 (1988).

[12] H. P. Saha (unpublished).

[13] C. N. Yang, Phys. Rev. **74**, 764 (1948).

[14] J. Cooper and R. N. Zare, in *Lectures in Theoretical Physics,* edited by S. Geltman, K. Mahathappa, and W. Britten (Gordon and Breach, New York, 1969), Vol. 11c, p. 317–337.

[15] C. Froese Fischer, Comput. Phys. Commun. **14**, 145 (1978).

[16] C. E. Moore, *Atomic Energy Levels,* Natl. Bur. Stand. (U.S.) Circ. No. 467 (U.S. GPO, Washington, D.C., 1958), Vol. III.